*Journal of the Geological Society*, *London*, Vol. **163**, 2006, pp. 127–142. Printed in Great Britain.

# Mesozoic extensional structures of the Fangshan tectonic dome and their subsequent reworking during collisional accretion of the North China Block

DAN-PING YAN[1,2,3,4], MEI-FU ZHOU[3], HONG-LIN SONG[1], GEN-HOU WANG[1] & MIN SUN[3]

[1]*State Key Laboratory of Geological Processes and Mineral Resources, China University of Geosciences, Beijing 100083, China*

[2]*Key Laboratory of Lithospheric Tectonics and Lithoprobing Technology of Ministry of Education, China University of Geosciences, Beijing 100083, China*

[3]*Department of Earth Sciences, the University of Hong Kong, Hong Kong SAR, China*

[4]*School of Earth Sciences and Resources, China University of Geosciences, Beijing 100083, China*

*(e-mail: yandp@cugb.edu.cn)*

**Abstract:** The Fangshan area, SW of Beijing, lies at the junction of the NNE-trending Taihang mountain range and the southeastern portion of the Yanshan intraplate orogenic belt and has undergone at least five stages of deformation. Mid- to late Triassic extensional deformation ($D_1$) is represented by the formation of the Fangshan tectonic dome during SE-directed extensional tectonics. This deformation was later modified by NNW-directed thrusting in the late Triassic ($D_2$) and WNW-directed thrusting in the late Jurassic ($D_3$). These $D_1$–$D_3$ structures were deformed by the arcuate Beiling syncline ($D_4$), which formed during the intrusion of the 133–128 Ma Fangshan pluton. $D_5$ deformation is represented by Cretaceous to Quaternary NNE-striking high-angle normal faults. The ages of these events demonstrate that the principal ENE-trending tectonic framework of the Yanshan intraplate orogenic belt was established mainly in the mid- to late Triassic (the Indosinian event). The Jurassic to Cretaceous Yanshanian deformation with thick-skinned thrusting was associated with intrusion of numerous plutons, and strongly modified the older structures. The tectonic evolution of the Fangshan tectonic dome was linked genetically with the collision of the North China Block and the Siberian Craton, and the later collision of the North and South China blocks.

The ENE-trending Yanshan intraplate orogenic belt has been known in China since the study by Wong (1929), and many subsequent studies have been carried out (e.g. Zheng *et al*. 1988; Davis *et al*. 1989, 2001; Hebei Bureau of Geology 1989, 1990; Liaoning Bureau of Geology and Mineral Resources 1989; Zhao *et al*. 1990; Beijing Bureau of Geology and Mineral Resources 1991; Shan *et al*. 1991; Faure & Natlin 1992; Wang 1996; Zhang 1996; Chen 1998; Zhang, C. *et al*. 2001; Darby & Ritts 2002) (Fig. 1). Although the geological and geophysical characteristics of the Yanshan belt are well known (Hebei Bureau of Geology 1989; Liaoning Bureau of Geology and Mineral Resources 1989; Beijing Bureau of Geology and Mineral Resources 1991), interpretations of its structural style and kinematics are controversial. For example, it is considered by some to represent a thick-skinned tectonic domain involving numerous thrust faults that cut steeply downward into the Archaean crystalline basement (Bao *et al*. 1983; Beijing Bureau of Geology and Mineral Resources 1991; Zhang 1996). This structural pattern is similar to that of the Laramide orogenic belt in the Rocky Mountains of the USA (Richard 1991; Robert 1998; Timothy & Stephen 1999; Martin 2003). However, numerous thin-skinned features, including thin-skinned folds and thrust faults, have also been identified (Song & Ge 1984; Shan *et al*. 1991; Wang 1996; Davis *et al*. 1998, 2001).

Previous studies have dealt largely with the Late Mesozoic deformation of the Yanshan belt (e.g. Faure & Natlin 1992; Davis *et al*. 1998, 2001; Darby *et al*. 2001). For example, in the northern part of the North China Block (Fig. 1), several metamorphic core complexes occur along the Yinshan–Yanshan mountain ranges. The metamorphic core complex at Hohhot (Fig. 1) has an Archaean basement core separated from Mesoproterozoic to Cretaceous cover rocks by a low-angle normal (detachment) fault. This was formed during a major period of SE-directed extension during Early Cretaceous time immediately following cessation of thrusting (*c*. 125 Ma) in the east–west-trending Yinshan fold-and-thrust belt (Davis *et al*. 2002). Similarly, the Yunmen metamorphic core complex (Fig. 1; Davis *et al*. 1996) and the quasi-metamorphic core complex (Fig. 1; Han *et al*. 2001) formed during mid- to late Cretaceous extension. These metamorphic core complexes, which lie within the Yanshan belt, represent a major period of intra-continental extension during Late Mesozoic time (Meng 2003; Meng *et al*. 2003). Although Late Palaeozoic to Early Mesozoic (Permian to Triassic) deformation is also known (Song & Ge 1984; Darby *et al*. 2001; Davis *et al*. 2001), its structural style and tectonic significance have not been investigated.

An Early Mesozoic period of extension is interpreted by the structural features recently identified within a number of extensional tectonic domes, including the Fangshan (Shan *et al*. 1991), Dushan (Yu & Zhang 1996), Malanyu (Chen 1999), Fuping and Zanfang domes (Lei *et al*. 1994; Niu *et al*. 1994), and several other possible extensional tectonic domes (Fu 1999). These domes together define a NE-trending extensional belt within the Yanshan and Taihang mountain ranges (Fig. 1). East China was a plateau during Mesozoic time and the mechanism of collapse of this plateau has been a matter of debate (Fan & Hooper 1991; Yin & Nie 1996; Zhang, Q. *et al*. 2001; Davis 2003; Fan *et al*. 2003). Thus the study of these tectonic domes may yield important insights into the understanding of the Mesozoic tectonic evolution of East China.

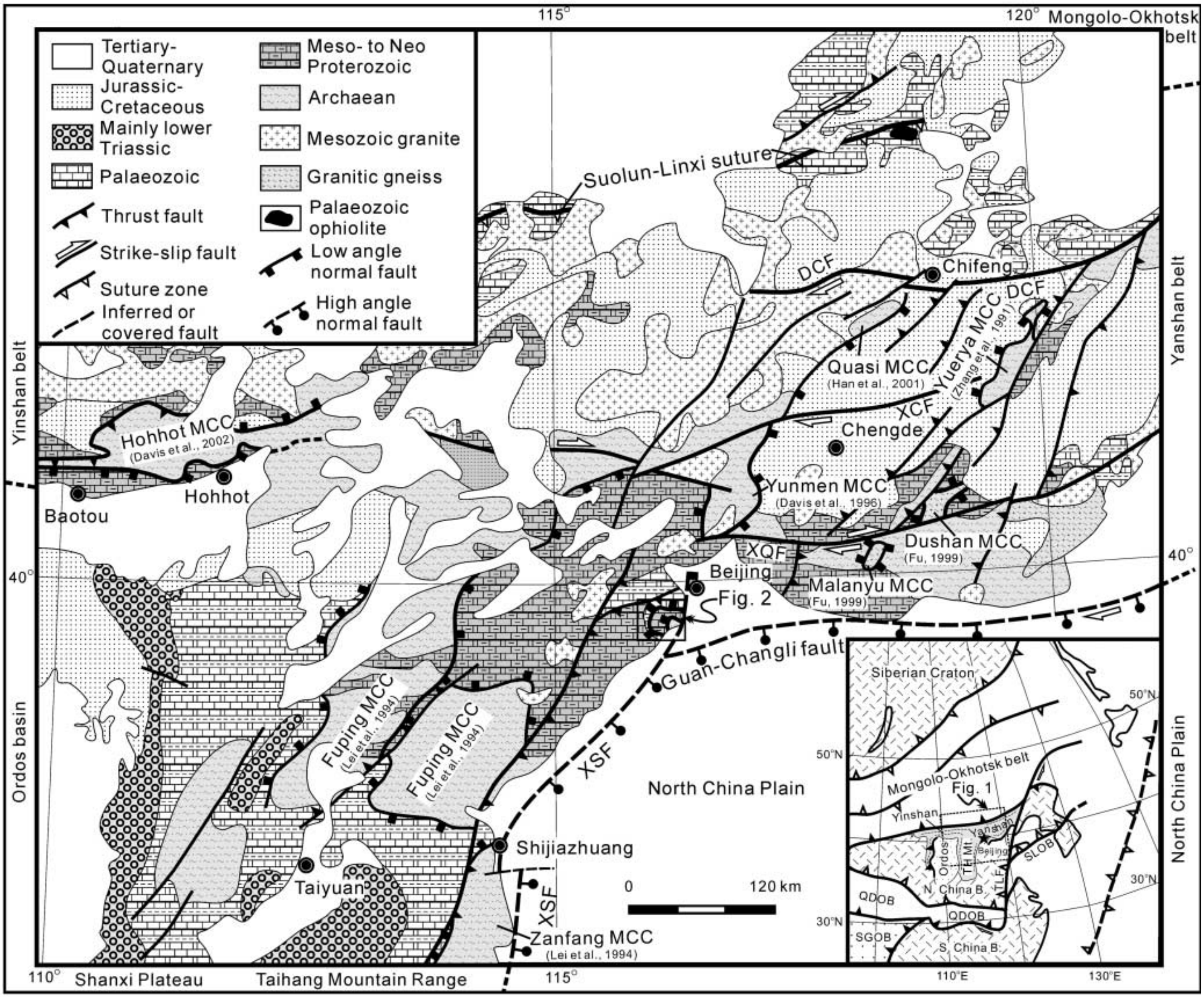


**Fig. 1.** Simplified geological map of the Yanshan mountains and adjacent areas in the North China Block. The location of the Fangshan area is shown (compiled from the following maps: Beijing Bureau of Geology and Mineral Resources 1991; Hebei Bureau of Geology 1989; Yin & Nie 1996; Chen 1998; Davis *et al*. 1998; Darby *et al*. 2001). QDOB, Qingling–Dabie Orogenic Belt; SGOB, Songpan–Ganzi Orogenic Belt; SLOB, Sulu Orogenic Belt; XQF, Xifengkou–Qinlong fault; XCF, Xianfa–Chicheng fault; DCF, Duolun–Chifeng fault; XSF, Xingtai–Shijiazhang fault; TLF, Tan–Lu fault.

The Fangshan tectonic dome is of particular interest because it lies at the junction of the NNE-trending Taihang tectonic belt and the ENE-trending Yanshan intraplate orogenic belt and has been overprinted by several periods of deformation (Fig. 2; Song & Ge 1984; Shan *et al*. 1991). The Fangshan tectonic dome was only recently recognized as an extensional dome. Previously, the Archaean basement rocks of the dome were considered to represent the contact metamorphic aureole of an intrusive Mesozoic pluton (Ho 1936; Guo 1985; Liu & Wu 1987). In addition, several periods of deformation and metamorphism have extensively modified the complex and obscured its true nature. During this study, we carried out extensive field mapping and obtained new geochronological data to determine the age and character of deformation within the Fangshan tectonic dome. In this paper, we discuss the age, lithology and structural styles of the Fangshan tectonic dome, and its tectonic significance in the context of the Yanshan and Taihang tectonic belts.

## Geological background

The North China Block is bounded by the Qinling–Dabie orogenic belt to the south, and by the Central Asian orogenic belt (Mongolo-Okhotsk accretionary belt) to the north (Fig. 1, inset). The Central Asian orogenic belt has undergone several stages of deformation, with ophiolites marking NNW-directed subduction during late Palaeozoic time along the Suolun–Linxi suture zone (Fig. 1; Zhang *et al*. 1984; Wang & Liu 1986; Nie *et al*. 1990; Zhao *et al*. 1990; Enkin *et al*. 1992; Yin & Nie 1996; Xiao *et al*. 2003). The Suolun–Linxi suture zone is composed of numerous top-to-the-north thrust faults and Palaeozoic ophiolites that were thrust southward onto Ordovician to Lower Permian strata (Wang *et al*. 1990; Wang 1996). This zone is intruded by Mesozoic granites and unconformably overlain by sporadic outcrops of Mesozoic strata (Fig. 1). Further to the north, the Mongolo-Okhotsk ocean opened in the Triassic, and began subducting to both the north and south during Late Triassic time (220–

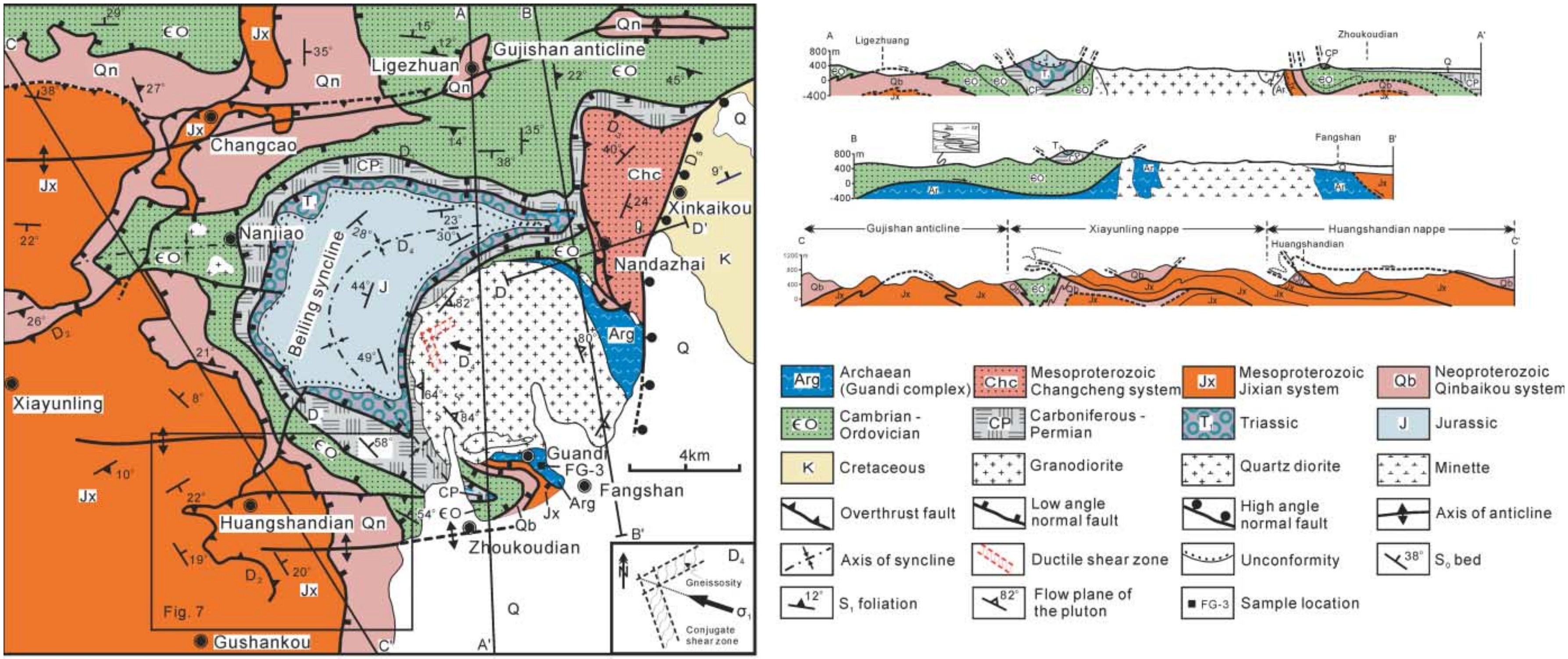


**Fig. 2.** Geological map of the Fangshan area, SW of Beijing (modified on the basis of Song *et al*. 1996).

208 Ma) (Yin & Nie 1996). The closure of this ocean and the final collision between the North China Block and the Siberian Craton, to form the Mongolo-Okhotsk accretionary belt, may have occurred during Late Jurassic time (Fig. 1, inset) (Ren *et al.* 1990; Yin & Nie 1996).

To the south, the *c.* 230 Ma indentation of the South China Block into the North China Block produced the Qinling–Dabie orogenic belt (e.g. Hacker *et al.* 1998; Chavagnac *et al.* 2001; Ayers *et al.* 2002), associated with dextral east–west-striking faults and the left-slip, NNE-striking Tan–Lu fault (Fig. 1, inset; Yin & Nie 1996). In the eastern North China Block, this indentation resulted in extensive north–south crustal shortening and subsequent intra-continental deformation (Yin & Nie 1996). This subsequent deformation resulted in the formation of a topographically high region, the North China Plateau, where little Triassic sediment was deposited and adakitic rocks were formed (Fan & Hooper 1991; Yin & Nie 1996; Zhang, Q. *et al.* 2001; Davis 2003; Fan *et al.* 2003; Meng 2003). During Jurassic time, continued westward displacement of the South China Block relative to the North China Block along the Tan–Lu fault led to WNW-directed movement of the southern North China Block and ESE-directed extrusion of the Yanshan intraplate orogenic belt (Zhang 1997).

The Yanshan intraplate orogenic belt, located at the northern margin of the North China Block, is the eastern segment of the ENE-trending Yanshan–Yinshan belt (Hebei Bureau of Geology 1989; Beijing Bureau of Geology and Mineral Resources 1991; Davis *et al.* 1998) (Fig. 1). It is separated from the North China Plain to the south by the concealed, high-angle normal Guan–Changli fault, which is marked by concentrated electrical isobath and gravity gradients (Hebei Bureau of Geology 1989). Within the Yanshan belt, numerous ENE-striking dextral-slip, transpressional faults, including the Duolun–Chifeng fault, Xianfa–Chicheng fault and Xifengkou–Qinlong fault, are related to multiple stages of deformation between the Palaeoproterozoic and the Mesozoic (Hebei Bureau of Geology 1989; Beijing Bureau of Geology and Mineral Resources 1991). In the central part of the North China Block, the NNE-trending Taihang mountain range was uplifted in the Cenozoic (Hebei Bureau of Geology 1990; Beijing Bureau of Geology and Mineral Resources 1991). This mountain range is separated from the North China Plain to the east by the Xingtai–Shijiazhang high-angle normal fault, also a concealed fault inferred from geophysical data and confirmed in drill holes (Hebei Bureau of Geology 1989). The mountain range gradually merges into the Shanxi Plateau to the west (Fig. 1).

The basement of the North China Block consists dominantly of middle to upper Archaean gneisses, granulites and migmatites, and is overlain by a variety of Mesoproterozoic to Triassic cover rocks, which are mostly undeformed (Hebei Bureau of Geology 1990; Beijing Bureau of Geology and Mineral Resources 1991; Kusky *et al.* 2004). The cover sequence includes Meso- to Neoproterozoic (*c.* 1850–800 Ma) shallow-water marine strata of variable thickness, Cambrian–Middle Ordovician shallow marine carbonates and Upper Carboniferous–Permian marine carbonates and terrestrial, coal-bearing clastic rocks. The Upper Permian rocks are unconformably overlain by Lower Triassic red-beds and conglomerates, which in turn, are unconformably overlain by Lower Jurassic–Cretaceous terrestrial volcanic and clastic deposits (Beijing Bureau of Geology and Mineral Resources 1991).

In the Fangshan area (Fig. 2), the rocks are similar to those in the rest of the North China Block (Fig. 3). The basement rocks consist of the Archaean Guandi complex, which is composed of crystalline rocks with an age of *c.* 2.5 Ga (see below). The Mesoproterozoic strata belong to the Changcheng and Jixian groups. The Changcheng group consists of clastic rocks whereas the Jixian group is composed of both fine-grained clastic and carbonate rocks that structurally overlie the Guandi complex. The Mesoproterozoic strata are conformably overlain by the Neoproterozoic–Lower Palaeozoic Qinbaikou group composed of clastic deposits with minor carbonates. Coarse-grained clastic rocks make up most of the Upper Palaeozoic, Triassic and Jurassic sequences, although the latter contains some interlayered coal beds (Fig. 3).

The Guandi complex and its overlying sedimentary strata are intruded by the Fangshan pluton (Fig. 2). This intrusion is composed of quartz diorite and granodiorite. The quartz diorite has yielded K–Ar biotite ages of $131.0 \pm 5.4$ and $132.7 \pm 0.12$ Ma, and K–Ar amphibole ages of $129.1 \pm 0.52$ and $132.8 \pm 0.12$ Ma (Beijing Bureau of Geology and Mineral Resources & China University of Geosciences 1988), and $^{40}Ar/^{39}Ar$ biotite ages of $133.0 \pm 0.9$ and $132.7 \pm 1.4$ Ma (Liu & Wu 1987). The granodiorite from this intrusion is dated at $128.5 \pm 1.5$ Ma (zircon U–Pb age) (Davis *et al.* 2001) and $127.7 \pm 5.1$ Ma (K–Ar biotite age) (Beijing Bureau of Geology and Mineral Resources & China University of Geosciences 1988). Thus the Fangshan pluton was emplaced at *c.* 130 Ma (128–133 Ma).

## Age of the Guandi complex

The first step in understanding the geology of the Fangshan tectonic dome is to distinguish between the metamorphic core and the later *c.* 130 Ma dioritic intrusion. The protolith and metamorphic ages of the core complex were previously unknown. Thus, we dated zircons from a sample of orthogneiss (FG-3; Fig. 2) from the inner core composed of plagioclase, microcline, amphibole, biotite and quartz.

### *Analytical techniques*

Isotopic analyses were performed on the sensitive high-resolution ion microprobe (SHRIMP II) in the Institute of Geology, Chinese Academy of Geosciences, Beijing. Zircon samples were mounted in epoxy and ground to approximately half their thickness to expose their centres. A piece of reference zircon SL13 from the Research School of Earth Science at the Australian National University, and several grains of the TEMORA standard (TEM; see Black *et al.* 2003) were also prepared in a separate mount. The analytical procedure is similar to that given by Compston *et al.* (1984). For zircon analyses, nine ion species of $Zr_2O^+$, $^{204}Pb^+$, $^{207}Pb^+$, $^{208}Pb^+$, $U^+$, $Th^+$, $ThO^+$ and $UO^+$ were measured on a single electron multiplier by cyclic stepping of the magnetic field, recording the mean ion counts of every seven scans. A primary ion beam of about 4.5 nA, and 10 kV $O^{2-}$ was used to measure a spot about 25–30 μm in diameter. Mass was analysed at a mass resolution of about 5400 (1% peak height). Inter-element fractionation in ion emission of zircon was corrected relative to the RSES references, using standard SL13 and TEMORA. The reproducibility of the TEMORA reference material was about 2%. The software SQUID 1.02 and ISOPLOT (Ludwig 2001) were used for data processing. The correction for initial lead (from $^{204}Pb$) was made using the Pb composition (Stacey & Kramers 1975) recommended by IUGS (1977). Uncertainties in ages are cited as 1σ, and the weighted average mean ages are quoted at 95% confidence limits.

### *Analytical results*

The results of the analyses are shown in Figure 4 and Table 1. Zircon grains from sample FG-3 show sector zoning with the characteristics of well-defined high-, intermediate- or low-U cores. Three analyses (FG3-5, 6 and 13) show a small degree of

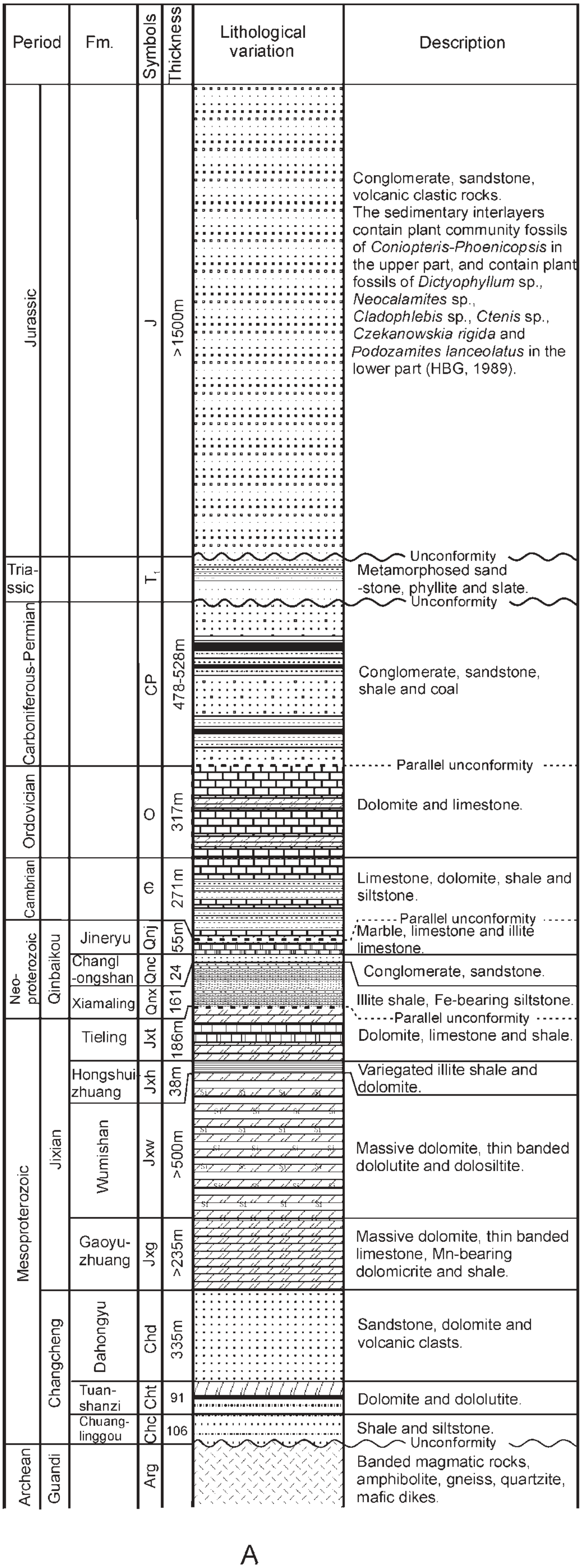


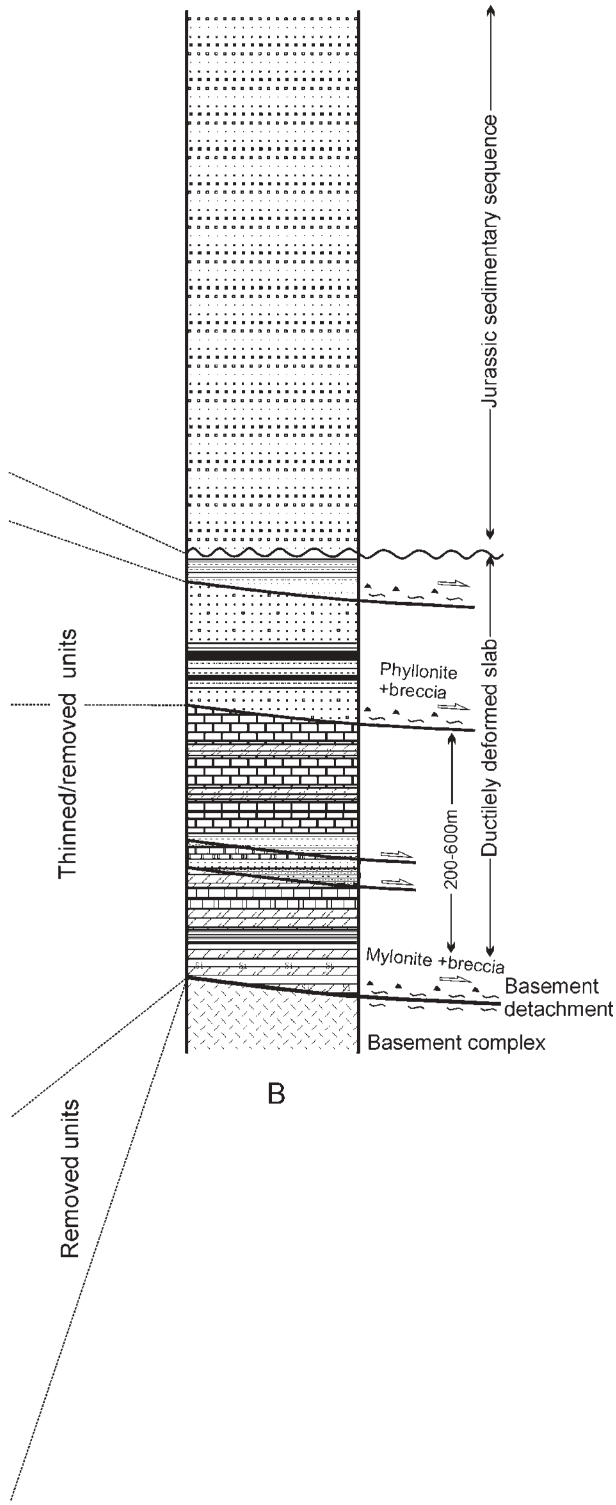


**Fig. 3.** Columnar section showing the lithologies, thicknesses and map symbols of the major sedimentary sequences in the Fangshan area. On the right is a modified section showing the sequence after thinning and removal of lithological units by detachment faulting.

Pb loss, leading to younger apparent $^{206}Pb/^{238}U$ ages. Five analyses are discordant and define a discordia line. These analyses together with six remaining concordant analyses yield an upper intercept $^{206}Pb/^{238}U$ age of $2521 \pm 20$ Ma and a lower intercept age of $681 \pm 140$ Ma (96% confidence), where the uncertainty is the 1σ error on the mean and the mean square weighted deviation (MSWD) is 1.4 (Fig. 4). The upper intercept age is considered the best estimate of the crystallization age, whereas the geological significance of the lower intercept age is uncertain because of its larger error. Therefore, the Guandi complex is interpreted as part of the Archaean basement.

## Geology and deformation of the Fangshan tectonic dome and surrounding areas

At least five generations of deformation were identified in the Fangshan tectonic dome and surrounding area. Formation of the Fangshan tectonic dome encompasses an early extensional phase of deformation ($D_1$), which was overprinted by four additional stages of deformation.

### *Early Mesozoic extensional deformation ($D_1$)*

An early Mesozoic extensional deformation was responsible for the initial formation of the Fangshan tectonic dome, which consists of two units (Fig. 3): a basement complex locally known as the Guandi complex and an overlying ductilely deformed slab of Mesoproterozoic, Neoproterozoic, Palaeozoic and Lower Triassic strata. After deformation, the Lower Triassic strata were unconformably overlain by Jurassic terrestrial deposits (section A–A′ in Fig. 2; Fig. 3a). These deposits contain abundant fossils including *Coniopteris–Phoenicopsis* in the upper part, and *Dictyophyllum* sp., *Neocalamites* sp., *Cladophlebis* sp., *Ctenis* sp., *Czekanowskia rigida* and *Podozamites lanceolatus* in the lower part, all of which indicate a Jurassic age (Hebei Bureau of Geology 1989) (Fig. 3a). Major detachment faults, interpreted as extensional in origin, separate the deformed slab from the basement complex and overlying cover unit. There are also numerous detachment faults within the middle slab (Wei & Song 1990; Shan *et al*. 1991) (Figs 2 and 3b).

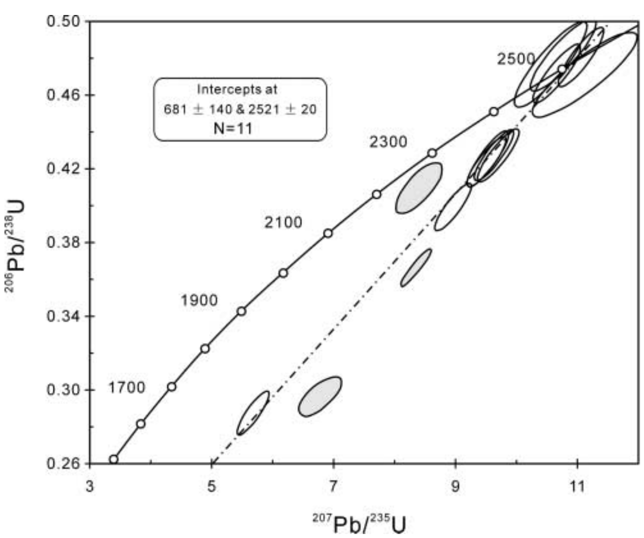


**Fig. 4.** SHRIMP zircon U–Pb isotopic concordia plot for the Guandi complex, Fangshan area, SW of Beijing.

**Table 1.** *SHRIMP U–Pb isotopic analyses for zircons from the Guandi complex*

| Spot | % $^{206}Pb_c$* | Ratios corrected common Pb† | | | | | | $^{206}Pb$ (ppm) | U (ppm) | Th (ppm) | Th/U | $^{206}Pb/^{238}U$ age (Ma) | $^{207}Pb/^{206}Pb$ age (Ma) | % Discordant |
|---|---|---|---|---|---|---|---|---|---|---|---|---|---|---|
| | | $^{206}Pb/^{238}U$‡ | ±% | $^{207}Pb/^{235}U$§ | ±% | $^{207}Pb/^{206}Pb$‖ | ±% | | | | | | | |
| FG3-1 | 0.01 | 0.4274 | 2.1 | 9.63 | 2.2 | 0.16346 | 0.40 | 98.4 | 268 | 135 | 0.52 | 2294 ± 41 | 2491.8 ± 6.7 | 8 |
| FG3-2 | 0.97 | 0.471 | 3.2 | 11.12 | 5.1 | 0.1713 | 4.0 | 3.09 | 8 | 4 | 0.53 | 2488 ± 66 | 2570 ± 66 | 3 |
| FG3-3 | 0.02 | 0.481 | 2.2 | 11.06 | 2.2 | 0.16697 | 0.53 | 48.7 | 118 | 82 | 0.71 | 2530 ± 45 | 2527.5 ± 9.0 | 0 |
| FG3-4 | 0.13 | 0.472 | 2.2 | 10.66 | 2.4 | 0.1639 | 0.95 | 42.7 | 105 | 62 | 0.61 | 2491 ± 45 | 2496 ± 16 | 0 |
| FG3-5 | 0.29 | 0.3655 | 2.2 | 8.35 | 2.4 | 0.1658 | 0.85 | 29.4 | 93 | 43 | 0.47 | 2008 ± 38 | 2515 ± 14 | 20 |
| FG3-6 | 0.58 | 0.2952 | 2.9 | 6.77 | 4.2 | 0.1663 | 3.0 | 3.82 | 15 | 6 | 0.42 | 1667 ± 43 | 2521 ± 50 | 34 |
| FG3-7 | 0.01 | 0.3992 | 2.1 | 8.96 | 2.2 | 0.16280 | 0.38 | 122 | 357 | 114 | 0.33 | 2165 ± 39 | 2485.0 ± 6.3 | 13 |
| FG3-8 | 0.10 | 0.4273 | 2.2 | 9.70 | 2.3 | 0.1646 | 0.69 | 43.4 | 118 | 60 | 0.53 | 2294 ± 42 | 2503 ± 12 | 8 |
| FG3-9 | 0.03 | 0.4255 | 2.3 | 9.53 | 2.3 | 0.16237 | 0.42 | 132 | 361 | 266 | 0.76 | 2285 ± 43 | 2480.5 ± 7.0 | 8 |
| FG3-10 | 0.14 | 0.4239 | 2.1 | 9.51 | 2.2 | 0.16268 | 0.45 | 75.5 | 207 | 92 | 0.46 | 2278 ± 41 | 2483.7 ± 7.6 | 8 |
| FG3-11 | 0.25 | 0.477 | 3.2 | 10.56 | 3.7 | 0.1607 | 1.8 | 6.37 | 16 | 16 | 1.08 | 2513 ± 67 | 2463 ± 30 | −2 |
| FG3-12 | 0.62 | 0.482 | 2.7 | 10.77 | 3.3 | 0.1620 | 1.9 | 6.43 | 15 | 16 | 1.06 | 2536 ± 56 | 2477 ± 32 | −2 |
| FG3-13 | 0.57 | 0.409 | 2.7 | 8.39 | 3.6 | 0.1489 | 2.4 | 5.82 | 16 | 20 | 1.27 | 2209 ± 51 | 2333 ± 41 | 5 |
| FG3-14 | 0.04 | 0.2875 | 2.7 | 5.68 | 3.0 | 0.1434 | 1.3 | 146 | 592 | 78 | 0.14 | 1629 ± 39 | 2269 ± 23 | 28 |

*$^{206}Pb_c$ % indicates percentage of total $^{206}Pb$ that is non-radiogenic.
†Errors are 1σ. Error in standard calibration was 0.48% (not included in above errors but required when comparing data from different mounts).
‡Common Pb corrected using measured $^{204}Pb$.
§Common Pb corrected by assuming $^{206}Pb/^{238}U$–$^{207}Pb/^{235}U$ age-concordance.
‖Common Pb corrected by assuming $^{206}Pb/^{238}U$–$^{208}Pb/^{232}Th$ age-concordance.

*Basement complex and basement detachment fault.* The Archaean Guandi complex crops out locally along the northern and southern margin of the Fangshan pluton (Fig. 2). The complex is composed of amphibolite, gneiss, quartzite and mafic dykes all metamorphosed under amphibolite-facies conditions with metamorphic mineral assemblages of almandine + biotite + plagioclase + quartz or amphibole + biotite + plagioclase + quartz. All of these rocks carry a gneissic foliation with variable strike and dip. Ductilely deformed rocks include felsic and amphibolitic blastomylonite and phyllonite.

Blastomylonite is mainly felsic with numerous lenses of amphibolite and defines a zone of a few centimetres to several tens of metres thickness. This zone is structurally below the detachment fault, separating the Archaean basement from the deformed slab (Figs 2, 3b and 5). It is characterized by ductile structures such as elongate quartz, plagioclase ribbons, alternating bands of dark and light minerals and a stretching lineation, and metamorphosed under amphibolite- to high greenschist-facies conditions with metamorphic mineral assemblages of kyanite + chloritoid + almandine + staurolite + biotite + muscovite + plagioclase (Fig. 5; Shan *et al*. 1991). The mineral lineations on the $S_1$ foliation indicate a NW–SE trend. Near the basement detachment fault, deformational features include S–C foliations, asymmetric pressure shadows and rotated porphyroclasts, all of which show a top-to-the-SE sense of shear (Fig. 5b and c).

The basement detachment fault is characterized by gouge and micro-breccia. Along the northern margin of the Fangshan pluton there is a 5–10 cm thick layer of gouge and micro-breccia at the top of the detachment fault (Figs 2 and 5a, b). Locally a sheet of schistose diorite along this fault (Fig. 5b) has a mylonitic foliation and is believed to be contemporaneous with the shear deformation (Song *et al*. 1996). This sheared diorite has a K–Ar amphibole age of $207 \pm 2$ Ma (Beijing Bureau of Geology and Mineral Resources & China University of Geosciences 1988), an age for the formation of the shear zone (Song *et al*. 1996).

Felsic dykes intruding the mylonite are interpreted to be contemporaneous with the adjacent granodiorite of the Fangshan pluton (section B–B′ in Fig. 2; Fig. 5b). There are abundant xenoliths of blastomylonite at the margin of the pluton, indicating that the intrusion postdates the shear zone.

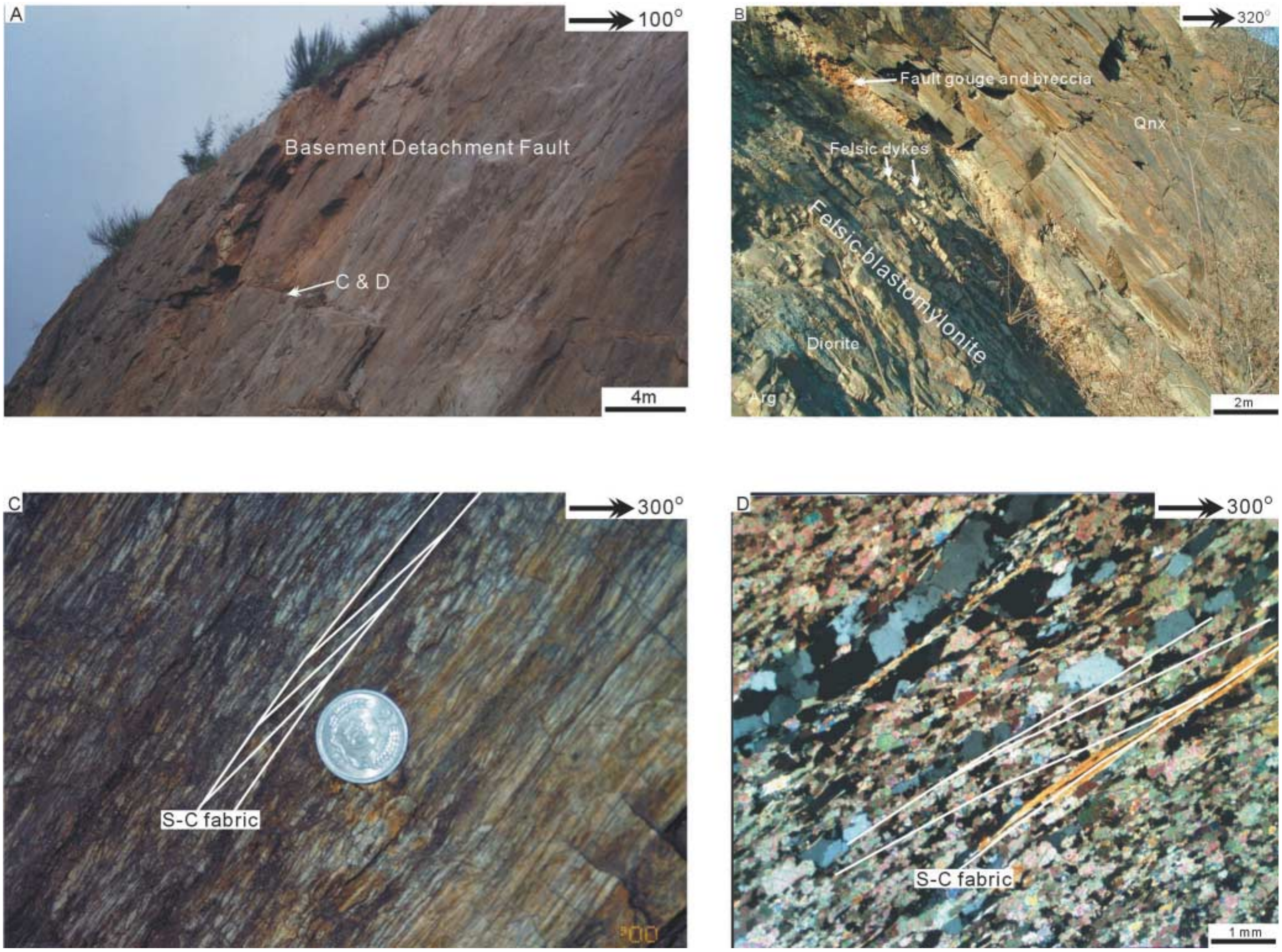


**Fig. 5.** Field photographs showing the basement detachment fault. (**a**) Blastomylonite, mylonitic foliation and mineral lineation on the foliation of the basement detachment fault in Guandi village, south of the Fangshan pluton (Fig. 2). (**b**) Mesoproterozoic Xiamaling Formation (Qnx) directly in contact with the Guandi complex (Arg), north of the Fangshan pluton. A basement detachment fault separates the core complex (Arg) from the Qnx and is associated with blastomylonitic rocks. A 5–10 cm thick layer of yellow fault gouge and micro-breccia is also visible. It should be noted that the diorite was involved in the deformation associated with the mylonitic foliation, but the felsic dykes intruded into the detachment fault and cut through the mylonitic foliation. (**c**, **d**) S–C fabric of a blastomylonitic rock in the footwall of the basement detachment fault.

Rocks in the hanging wall of the basement detachment fault have a foliation ($S_1$) parallel to the fault. Near the detachment fault, mylonitic rocks or micaschist have a foliation ($S_1$) parallel to the lithological boundary marked by a carbonaceous schist layer ($S_0$). The micaschist also forms small-scale recumbent folds with NE-trending axes. The detachment fault is at a small angle to the hanging-wall bedding layers (Figs 2 and 5b) (Song *et al*. 1996).

Mesoproterozoic, Neoproterozoic or Lower Palaeozoic strata of the middle slab are locally in direct contact with the amphibolitic blastomylonites of the footwall of the detachment fault (Fig. 2). Parts of the Mesoproterozoic and Jixian group are missing and have either been thinned or selectively removed by faulting (Fig. 3b).

*Ductilely deformed slab.* The ductilely deformed slab (Figs 3 and 7), separated from the basement complex by the basement detachment fault, consists of Mesoproterozoic, Neoproterozoic, Palaeozoic and Lower Triassic sedimentary sequences that crop out around the basement complex (Fig. 2). These sequences have undergone low to middle greenschist-facies metamorphism with metamorphic mineral assemblages of sericite + epidote + actinolite + plagioclase + chlorite + quartz, but original sedimentary structures are well preserved. Within the slab, there are pervasive intrafolial recumbent folds of the original bedding layers with amplitudes and wavelengths of variable scales (Fig. 7). The axial planar cleavage of the recumbent folds represents development of a penetrative foliation $S_1$ (Fig. 7a, b, d, e, h and i). Incompetent layers in the sequence formed ductile shear zones with phyllonite (Fig. 7b and e). The Meso- to Neoproterozoic, Palaeozoic and Lower Triassic units within the sequence were thinned or selectively removed by numerous detachment faults with top-to-the-SE sense of shear, as indicated by the overturned direction of the recumbent and sheath folds (Figs 3b and 7a–d, g, h). Mineral lineations on the $S_1$ foliation and the axes of sheath folds trend between 310 and 325° on the southwestern side of the Fangshan pluton (Fig. 7c–e), and between 105 and 125° on the northern margin (Fig. 7f–h). The extension direction coincides with the mineral lineation on the mylonite foliation of the basement detachment, which has a top-to-the-SE sense of shear if the $S_1$ foliation is restored to horizontal (assuming that the strata were horizontal before the subsequent deformations).

## *Subsequent deformation*

The early extensional deformation ($D_1$) was followed by two stages of thrust faulting ($D_2$ and $D_3$), formation of the arcuate Beiling syncline ($D_4$), and late-stage normal faulting ($D_5$).

*Western overthrust system ($D_2$).* The western overthrust system includes the Huangshandian, Changchao and Xiayunling nappes in the western part of the mapped area (Ge & Ren 1990) (section C–C' in Fig. 2; Figs 6 and 8).

In the footwall of the Huangshandian thrust fault, a narrow band of the Qinbaikou group of varying thickness forms the core of a syncline, which appears as a recumbent fold with an axial plane dipping to the SE (section C–C′ in Fig. 2; Figs 6 and 8). In the normal limb of the syncline, ductile shear zones with S–C fabric and subhorizontal $S_1$ foliation, which can be traced continuously to the detachment near the core complex (Shan *et al*. 1991), were preserved and involved in the Huangshandian thrust system (Fig. 8a and b), and show that the folded surface is the $S_1$ foliation that was formed during the earlier stage of extensional tectonics.

Thrust faults, which strike at N75–80°E, formed along the overturned limbs of synclines. To the east, the Huangshandian thrust faults cut through the $D_1$ detachment fault, and folded the detachment fault into the broad Zhoukoudian anticline (Figs 2 and 6). The thrust faults cut through the overturned limb of the syncline with a steep dip and formed a ramp in the northernmost outcrop, whereas they developed along the subhorizontal $S_1$ foliation and formed the flat to the south (sections in Fig. 6). Mineral lineations of calcite fibres on the thrust faults suggest a displacement direction of 340–350°.

A thicker band of the Jixian group forms the core of the isoclinal anticline in the hanging wall (Figs 6 and 8). Inverted stromatolites within the Wumishan Formation are top downward towards the NW, indicating the overturned limb of the recumbent fold (Fig. 8a and c). The anticline axis trends N75°–80°E, whereas the overturned-to-the-NW facing direction of the recumbent fold suggests that the direction of thrusting was 340–350° (section C–C′ in Fig. 1). The thrusting did not affect the Archaean basement and appears to result from a thin-skinned style of deformation.

The Xiayunling nappe is located north of the Huangshandian nappe (Fig. 2; section C–C′ in Fig. 2). The footwall of the thrust fault is composed of a narrow syncline with Cambrian to Ordovician strata exposed in the core and an inferred broad anticline with Proterozoic strata of the Jixian and Qinbaikou groups in the core. The thrust fault, which formed along the overturned limb of the isoclinal anticline of hanging wall, has a steep dip (>45°) at the western side, but is subhorizontal to the east, and therefore has a flat-ramp geometry (Shan *et al*. 1991). The structural styles are similar to those of the Huangshandian nappe (section C–C′ in Fig. 2). On the cross-section C–C′ in Figure 2, the magnitude of slip of the thrust fault is estimated to be about 5 km.

The Xiayunling thrust fault displaced the hanging-wall rocks to the NW (310–318°) based on the vergence of the recumbent anticline and calcite fibre lineations on the fault surface. This direction is consistent with the mineral stretching lineation (312–318°) within the mylonite along the fault (Shan *et al*. 1991). The overthrust fault, which is overlain unconformably by Jurassic strata in the Beiling syncline (see below), cross-cuts the $D_1$ detachment faults and the associated ductilely deformed slab, indicating an age of later than $D_1$ and earlier than Jurassic.

The Changcao nappe, NW of the Fangshan tectonic dome, consists of the Qinbaikou group and Cambrian–Ordovician strata in the footwall, and an east–west-striking thrust fault formed along the north limb of the Gujishan anticline, which belongs to the hanging wall (Fig. 2). The thrust fault, extending to the west of Ligezhuang, cross-cuts the $D_1$ detachment fault, and terminates in the broad Gujishan anticline (Fig. 2).

*Nandazai thrust ($D_3$).* NE of the Fangshan tectonic dome (Figs 2 and 9), the footwall of the Nandazai thrust fault comprises Palaeozoic strata with well-preserved structural characteristics of the ductilely deformed slab ($D_1$). The NNE-striking bow-shaped

**Fig. 6.** A geological map showing the Huangshandian nappe with cross-sections E–E′, F–F′ and G–G′ (compiled on the basis of Shan *et al*. 1991). The stereonet plots (lower hemisphere projections) of mineral lineations on the $S_1$ foliation (lower left) and $S_2$ (upper right) should be noted.

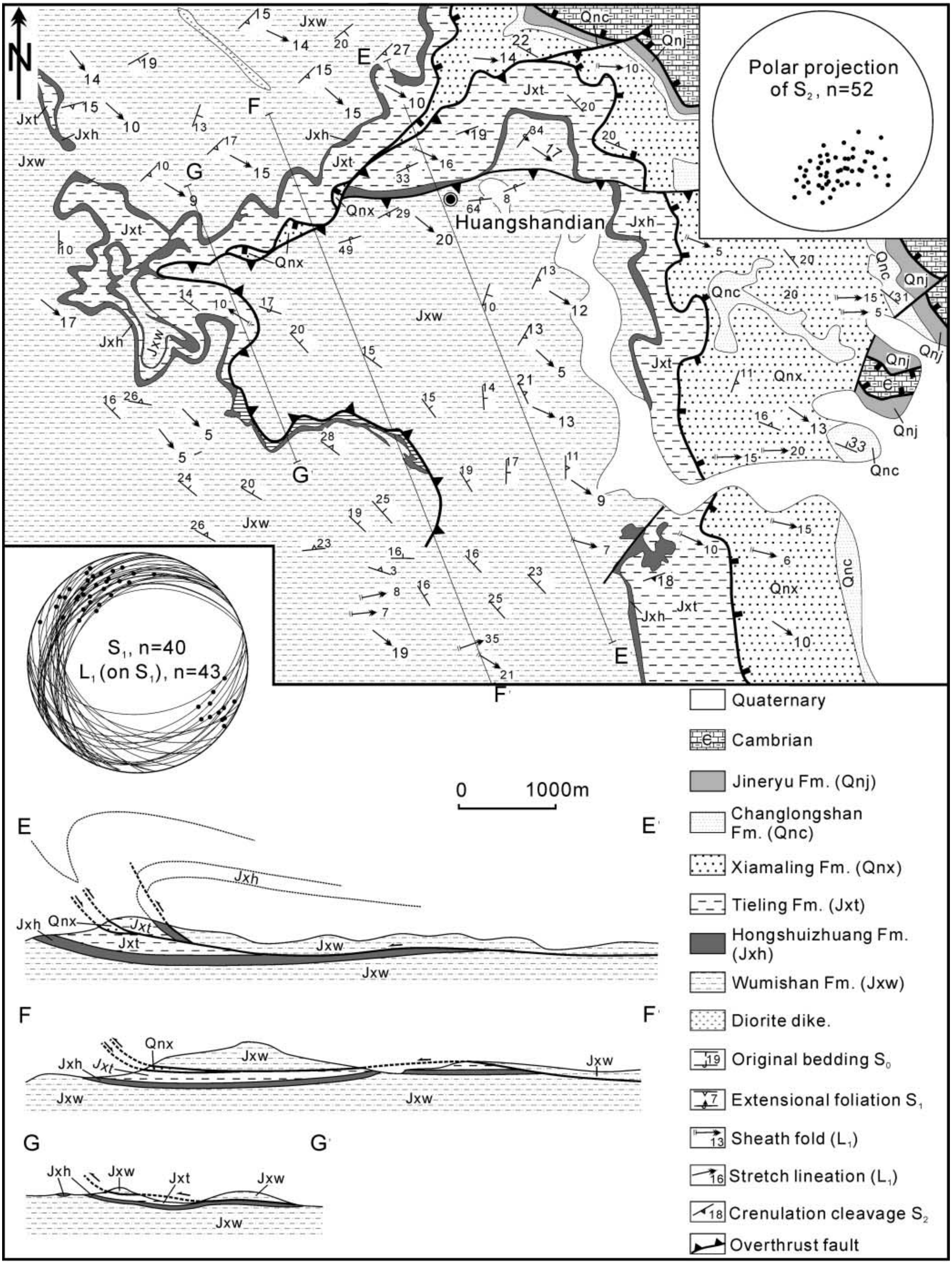
N
Polar projection
of S₂, n=52
S₁, n=40
L₁ (on S₁), n=43
Huangshandian
Jxw
Jxt
Jxh
Qnx
Qnc
Qnj
0 1000m
E
E'
F
F'
G
G'
Quaternary
Cambrian
Jineryu Fm. (Qnj)
Changlongshan
Fm. (Qnc)
Xiamaling Fm. (Qnx)
Tieling Fm. (Jxt)
Hongshuizhuang Fm.
(Jxh)
Wumishan Fm. (Jxw)
Diorite dike.
Original bedding S₀
Extensional foliation S₁
Sheath fold (L₁)
Stretch lineation (L₁)
Crenulation cleavage S₂
Overthrust fault

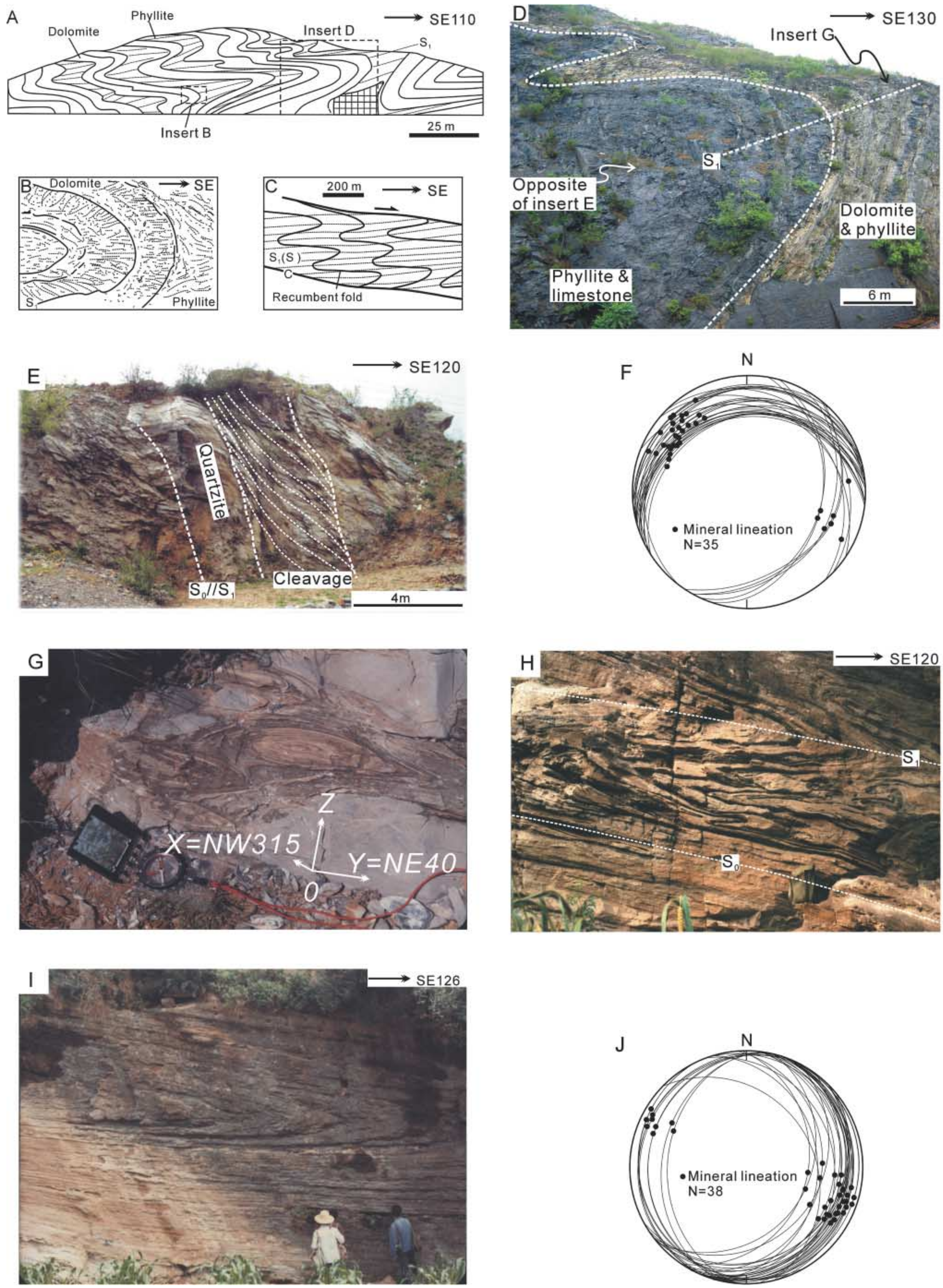
A
Phyllite
Dolomite
Insert D
SE110
$S_1$
Insert B
25 m
B
Dolomite
SE
$S_1$
Phyllite
C
200 m
SE
$S_1$(S)
C
Recumbent fold
D
SE130
Insert G
$S_1$
Opposite of insert E
Dolomite & phyllite
Phyllite & limestone
6 m
E
SE120
Quartzite
$S_0$//$S_1$
Cleavage
4m
F
N
Mineral lineation
N=35
G
Z
X=NW315
Y=NE40
0
H
SE120
$S_1$
$S_0$
I
SE126
J
N
Mineral lineation
N=38

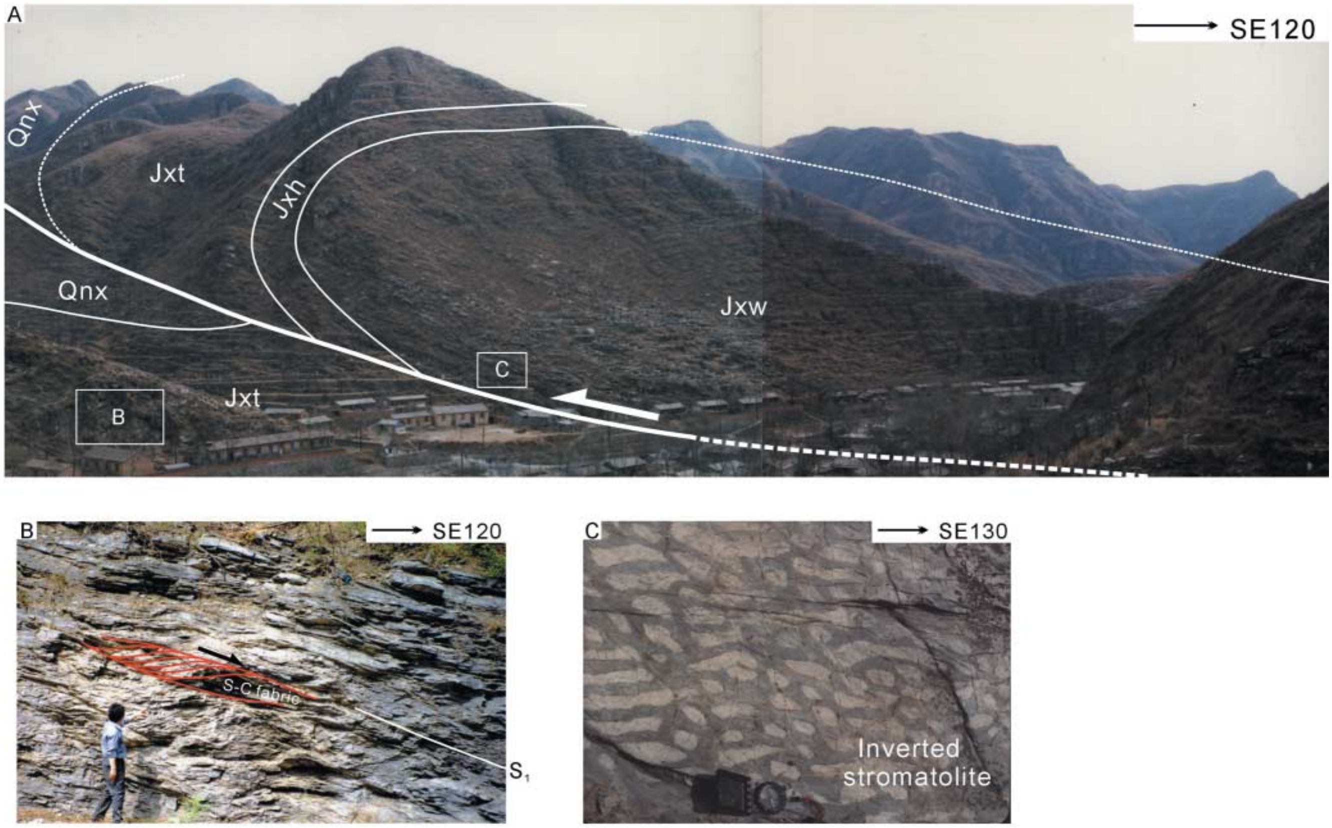


**Fig. 8.** Field photographs of the Huangshandian area (for location see Fig. 2). (**a**) A NW-directed recumbent fold in the hanging wall of the SE-dipping Huangshandian thrust fault. (**b**) A ductile shear zone in the Tieling formation with carbonate mylonites and a S–C fabric ($S_1$ foliation), involved in the overthrust deformation, indicating that earlier fabrics are related to top-to-the-SE detachment faulting. (**c**) Inverted stromatolites within the Wumishan formation on the overturned limb of the recumbent fold. Abbreviations as in Figure 6.

Nandazai thrust fault, which dips gently to the ESE, cuts through the detachment faults and the $S_1$ foliation of the ductilely deformed slab. Breccia, fault gouge and slickenlines are developed on the surface of the thrust fault. To the east, the hanging wall comprises the Mesoproterozoic Changcheng group (Chc) disposed in an asymmetrical anticline with an axial plane that is inclined steeply to the east (Shan *et al*. 1991) (Figs 2 and 9). Therefore, the hanging wall is interpreted as an allochthonous nappe, which was thrust westward onto Palaeozoic rocks along the Nandazhai fault (Beijing Bureau of Geology and Mineral Resources & China University of Geosciences 1988; Shan *et al*. 1991). The Nandazai thrust fault, cross-cutting the northeastern limb of the Beiling syncline, was intruded by the apophyses of the Fangshan pluton (Shan *et al*. 1991; Song *et al*. 1996) (Figs 2 and 9).

West of Changcao, a NNE-striking fault thrust the Jixian group over the Qingbaikou group and Lower Palaeozoic strata, and is associated with a recumbent anticline in the hanging wall. This fault, which has a structural style and deformation age identical to the Nandazai nappe, cross-cuts the Changcao nappe, and therefore formed later than the $D_2$ deformation (Fig. 2).

*Composite Beiling syncline ($D_4$).* The Beiling syncline, NW of the Fangshan pluton, has an arcuate trace (Fig. 2). Jurassic strata form the core of the syncline, which appears as a broad fold, whereas the Triassic and the older sequences appear as a tight fold, which is consistent with the footwall syncline ($D_2$) of the Xiayunling nappe (Fig. 2 and section A–A′). The disharmonic structural style implies a polyphase origin for the Beiling syncline, and the Beiling syncline fold axis is itself folded along an approximately east–west-trending axis.

Within the Fangshan pluton, a penetrative foliation is well

**Fig. 7.** Field photographs and sketches showing deformation within the ductilely deformed slab at Gushankou and Ligezhuang (for location see Fig. 2). (**a**) A large-scale recumbent fold at Gushankou involving dolomite, limestone and phyllite of the Wumishan formation (Qnx). (**b**) A subharmonic parallel fold (type IB) in competent dolomite, compared with a type III fold in incompetent phyllite (see Ramsay & Huber 1987). (**c**) A ductile shear zone (inferred from several outcrops in Gushankou area), which has a top-to-the-SE sense of shear. (**d**) Hinge zone of the large-scale recumbent fold at Gushankou involving dolomite, limestone and phyllite of the Wumishan formation. (**e**) Cleavages within the phyllite of the recumbent fold indicate a top-to-the-SE sense of shear. (**f**) Stereonet plot (lower hemisphere projection) of mineral lineations and $S_1$ foliation from the locality shown in (**e**), indicating the SE–NW orientation of the principal strain. (**g**) Sheath fold noses in the *yz* section of the $D_1$ strain ellipsoid. (**h**) $D_1$ recumbent folds with axial-planar $S_1$ developed in the Qinbaikou group in Nanjiao (for location see Fig. 2). (**i**) $D_1$ large-scale recumbent fold developed in marbles of the Neoproterozoic Jineryu Formation in Ligezhuan (for location see Fig. 2). (**j**) Stereonet plot (lower hemisphere projection) of mineral lineations and $S_1$ foliation from the locality shown in (**i**) indicate the SE–NW orientation of the principal strain direction.

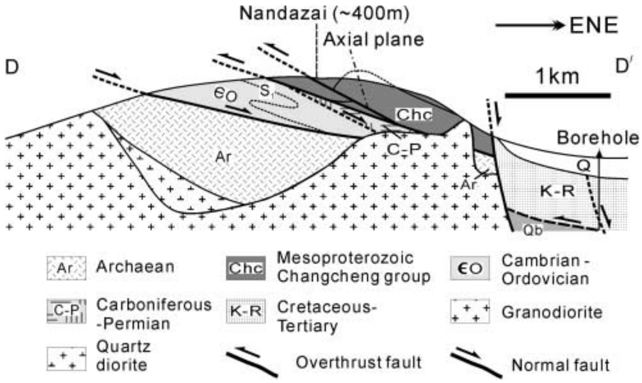


**Fig. 9.** D–D′ cross-section of the Nandazai thrust system; section location is shown in Figure 2.

developed on the western side, where the rock becomes gneissic and the xenoliths change from angular to disc-shaped (Zhang & Li 1991; Song *et al*. 1996). The aspect ratio of the xenoliths ranges from 10 to 50 in the centre of the zone. Two sets of vertical ductile shear zones, about 10 m wide, are present in this zone, along which the rocks are completely mylonitized. The bisectrix of the obtuse angle of the conjugate shear zones is parallel to the contraction direction and coincides in orientation with the normal of the syndeformational foliation (gneissosity) (Fig. 2, inset). The foliation is vertical and strikes NNE. One set of vertical shear zones strikes NE with a dextral strike-slip sense of shear; the other strikes NNW with a sinistral strike-slip sense of shear (Fig. 2). These structures are interpreted as the result of late-magmatic cooling during which the rocks were deformed. Therefore, they indicate that the direction of intrusion was from the SSE upward to the NNW. Deformation associated with emplacement of the intrusion resulted in further tightening of the $D_2$ Beiling syncline to form the composite $D_4$ fold (Song 1996; Song *et al*. 1996).

*High-angle normal fault system ($D_5$).* A high-angle normal fault system in the eastern part of the Fangshan tectonic dome separates the North China Plain to the east from the Proterozoic to Palaeozoic strata to the west (Figs 1 and 2). This fault system strikes NNE and dips 70–85° to the SSE. The North China Plain, the hanging wall of the fault, consists of Cretaceous to Quaternary sedimentary rocks (Fig. 9). This fault system formed as a result of Cretaceous to Quaternary extension and was responsible for uplift of the Taihang mountain range (Meng 2003; Meng *et al*. 2003).

## Discussion

### *Early Mesozoic SE-directed extension and its possible mechanism*

The Fangshan tectonic dome is a key element within the Yanshan intraplate orogenic belt and the Taihang tectonic belt but its true nature has long been a matter of debate. The confusion stemmed from the intrusion of the Fangshan pluton into the inner core of the Fangshan tectonic dome, which led earlier workers to interpret the entire body as a stock surrounded by a zone of contact metamorphism. However, the pluton is clearly intruded into older basement rocks (the Guandi complex), which are dated at 2.5 Ga and interpreted as the core of the Fangshan tectonic dome. The interpretation of the Fangshan tectonic dome as an extensional dome is also based on thinning and removal of key strata along original low-angle detachment faults, the sharp upward decrease in metamorphic grade from amphibolite facies to lower greenschist facies across these faults, and the exhumation of a metamorphic core.

Our detailed structural study reveals that the Fangshan tectonic dome was formed during Mid- to Late Triassic time, because Lower Triassic strata were involved in the ductile deformation, but the complex is overlain unconformably by Jurassic strata (Figs 2 and 3). Diorite dykes with a K–Ar age of 207 Ma in the basement detachment fault were involved in the mylonitic deformation (Beijing Bureau of Geology and Mineral Resources 1991; Song 1996; Song *et al*. 1996) (Fig. 5b). Exhumation of the Fangshan tectonic dome was associated with the $D_1$ deformation, suggesting a SE-trending principal extension direction during Mid- to Late Triassic time.

On a regional scale, the Dushan, Malanyu, Yuerya, Zanfang and Fuping domes in the eastern part of the Yanshan intraplate orogenic belt and the Taihang mountain range (Yu & Zhang 1996; Chen 1999; Fu 1999) are structurally similar to the Fangshan tectonic dome (Fig. 1). All of these domes have Archaean to Early Proterozoic granitic gneisses or gneissic rocks in their cores, and all have detachment faults with ductile deformation showing a top-to-the-SE extensional sense of shear. Granite intrusions within the Dushan dome (Fig. 1) are dated at $222 \pm 4$ and $223 \pm 2$ Ma (SHRIMP U–Pb, zircon) (Luo *et al*. 2003) and $239 \pm 1.3$ Ma ($^{40}Ar/^{39}Ar$, amphibole) (Zhang *et al*. 1991). The extension is interpreted to have occurred contemporaneously with emplacement of these granite intrusions at around 220 Ma.

The Fangshan, Dushan, Malanyu, Zanfang and Fuping domes form an extensional belt trending approximately NE and record major top-to-the-SE-directed extension during the Early Mesozoic. This age of extension within the North China Block coincides well with the opening and subsequent subduction of the Mongolo-Okhotsk ocean underneath the North China Block during the Triassic (Zhang *et al*. 1984; Wang & Liu 1986; Nie *et al*. 1990; Zhao *et al*. 1990; Yin & Nie 1996; Van der Voo *et al*. 1999; Zorin 1999; Badarch *et al*. 2002).

On the other hand, some metamorphic core complexes extending from west to east represent a period of major extensional tectonics during the Late Mesozoic (mainly late Jurassic to early Cretaceous) (Davis *et al*. 1996, 1998, 2002; Han *et al*. 2001). This extension was explained as a result of the final closure of the Mongolo-Okhotsk ocean and its subduction beneath the Northern China Block (Darby *et al*. 2001; Davis *et al*. 2001). This extension also resulted in lithospheric thinning of the North China Plateau (Fan & Hooper 1991; Yin & Nie 1996; Zhang, Q. *et al*. 2001; Davis 2003; Fan *et al*. 2003; Meng 2003). The Yanshanian orogenic belt involved two major periods of extension.

### *Tectonic significance of the post-extensional deformation*

The first post-extensional deformation ($D_2$) involved thin-skinned, north-directed thrust faulting and associated folding (Yan *et al*. 2003). The deformation is pre-Jurassic in age because these structures are unconformably overlain by Jurassic strata (Song & Ge 1984; Beijing Bureau of Geology and Mineral Resources & China University of Geosciences 1988). The second deformation ($D_3$) also involving thrust faulting has displaced the Changcheng group westward onto Lower Palaeozoic strata. These faults occurred in the late Late Jurassic because they cut the $D_2$

overthrust fault in the Nandazai and Changcao areas (Fig. 2), but were cross-cut by the Fangshan pluton (Fig. 9).

The $D_4$ deformation is associated with the emplacement of the Fangshan pluton at *c*. 130 Ma (Liu & Wu 1987; Davis *et al*. 2001). This intrusion resulted in the formation of the composite Beiling arcuate syncline. The Cenozoic NNE-striking, high-angle normal faults separate the Taihang mountain range from the North China Plain and mark the final deformation ($D_5$) in the region.

The recognition of these five generations of deformation is significant for understanding the regional geology and the origin of the Yanshan intraplate orogenic belt. They define the tectonic framework of the Fangshan area. ENE-trending structures of the Yanshan intraplate orogenic belt consistent with the Fangshan segment were formed by $D_1$ and $D_2$ deformation in pre-Jurassic time. The NNE-trending faults formed during the Late Cretaceous to present and were related to the uplift of the Taihang mountain range.

Here we propose a model for the tectonic evolution, related to subduction and collision between the North China Block and Mongolo-Okhotsk oceanic plate, and between the North China Block and South China Block, to explain the formation and subsequent deformation of the Fangshan tectonic dome.

Opening and subsequent SE-directed subduction of the Mongolo-Okhotsk oceanic plate during the Triassic time resulted in anatexis and thermal uplift flow (Holk & Taylor 1997), which was in turn responsible for the SE-directed extensional tectonics associated with the exhumation of the tectonic domes within the North China Block (Fig. 10a). Similar cases have also been described from British Columbia (Holk & Taylor 1997) and Australia (Little *et al*. 1992).

The $D_2$ deformation represents a period of north–south compressional deformation during Late Triassic time, which formed the ENE-striking thrust faults and folds. This deformation is a consequence of the intra-continental deformation resulting from the collision between the South China Block and North China Block and the subsequent extensive north–south crustal shortening within the North China Block (e.g. Yin & Nie 1996; Hacker *et al*. 1998; Chavagnac *et al*. 2001; Ayers *et al*. 2002).

A system of top-to-the-west directed thrust faults ($D_3$) formed on the western margin of the North China Plateau probably as a result of the interaction of the sinistral Tan–Lu fault and the dextral Xifengkou–Qinlong, Xianhua–Chicheng and Duolun–Chifeng faults within the Yanshan belt (Zhang, C. *et al*. 2001) (Figs 1 and 10c). This deformation was associated with a strongly thickened crust in the eastern North China Block (North China Plateau), which resulted in the NNW-directed movement of the southern North China Block and ESE-directed extrusion of the Yanshan belt (Fan & Hooper 1991; Zhang, Q. *et al*. 2001; Fan *et al*. 2003; Meng 2003) (Fig. 10c).

The composite Beiling syncline ($D_4$) was associated with the emplacement of the Fangshan pluton, coeval with large-scale magmatic activity elsewhere within the Yanshan belt and the Taihang mountain range. Therefore, it was coeval with the gravitational collapse of orogenically thickened crust in concordance with the development of isolated metamorphic core complexes identified by Davis *et al*. (1996, 1998, 2002), Darby *et al*. (2001) and Han *et al*. (2001). The deformation and magmatic activity occurred in the late Jurassic to early Cretaceous (Beijing Bureau of Geology and Mineral Resources 1991; Ren *et al*. 2002; Meng 2003; Meng *et al*. 2003). In addition, large-scale crustal thinning occurred in the North China Block at this time (Meng 2003; Meng *et al*. 2003), but the Yanshan intraplate orogenic belt remained in a compressional state because of the collision between the Siberian plate and the North China Block to form an east–west-trending orogenic belt (Fig. 10d).

Continued crustal thinning ($D_5$) from the Late Cretaceous to the present resulted from the successive gravitational collapse of orogenically thickened crust of the North China Block, and led to the formation of NNE-trending intra-continental rifts in the eastern North China Block (Gilder *et al*. 1991; Ren *et al*. 2002; Meng 2003; Meng *et al*. 2003). These intra-continental rifts formed a graben–horst combination separated by a high-angle normal fault, and later uplift of the Taihang mountain range formed the interfluve between the North China Plain and Taihang mountain range (Fig. 10e).

## Conclusions

Mid- to late Triassic extensional deformation ($D_1$) in the Fangshan area is represented by the formation of the Fangshan tectonic dome and was overprinted by NNW-directed thrusting in the Late Triassic ($D_2$) and Late Jurassic ($D_3$). These structures were modified by the intrusion of the 133–128 Ma Fangshan pluton ($D_4$), and cut by Cretaceous to Quaternary NNE-striking high-angle normal faults ($D_5$). Early Mesozoic subduction of the Mongolo-Okhotsk oceanic plate from north to south resulted in the $D_1$ extensional tectonics and produced the Fangshan tectonic dome. Collision between the South China Block and North China Block along the Qingling–Dabie–Sulu suture zone was responsible for the $D_2$ and $D_3$ thrust fault systems. The gravitational collapse of orogenically thickened crust was coeval with the development of isolated metamorphic core complexes during Late Jurassic to Early Cretaceous, and was probably responsible for the uplift of the Taihang mountain range during the Late Cretaceous. These tectonic events demonstrate that the major east–west-trending tectonic framework of the Yanshan intraplate orogenic belt was established before the Jurassic (mainly in the Triassic), corresponding to the Indosinian event in China.

This study was supported by the Nature Science Foundation of China (research grants 40472106 and 40434011 to D.-P.Y.; and outstanding young researcher award 40129001 to M.-F.Z., with a matching fund from The University of Hong Kong) and by the Research Grant Council of Hong Kong (HKU7124/02P). We are grateful to L. Ratschbacher and P. T. Robinson for their constructive reviews that helped to improve the paper. We have benefited from helpful discussions with Zhaoren Fu, Changhou Zhang and G. A. Davis during the last decade, and from the laboratory assistance of Yanbin Wang and Xiaoping Xia. We appreciate thorough reviews by R. Strachan, T. Kusky and an anonymous referee, whose insights helped to improve this manuscript.

## References

AYERS, J.C., DUNKLE, S., GAO, S. & MILLER, C.F. 2002. Constraints on timing of peak and retrograde metamorphism in the Dabie Shan Ultrahigh-Pressure Metamorphic Belt, east–central China, using U–Th–Pb dating of zircon and monazite. *Chemical Geology*, **186**, 315–331.

BADARCH, G., CUNNINGHAM, W.D. & WINDLEY, B.F. 2002. A new terrane subdivision for Mongolia: implications for the Phanerozoic crustal growth of Central Asia. *Journal of Asian Earth Science*, **21**, 87–110.

BAO, Y., XIE, D., CHEN, Z. & MU, B. 1983. On the Yanshanian movement in Beijing region. *Acta Geologica Sinica*, **57**, 195–204 (in Chinese with English abstract).

BEIJING BUREAU OF GEOLOGY AND MINERAL RESOURCES 1991. *Regional Geology of Beijing Municipality.* Ministry of Geology and Mineral Resources, Geological Memoirs, Series 1, **27**, (in Chinese with English abstract).

BEIJING BUREAU OF GEOLOGY AND MINERAL RESOURCES & CHINA UNIVERSITY OF GEOSCIENCES 1988. *Regional and Mineral Resource Geology of the Zhoukou-*

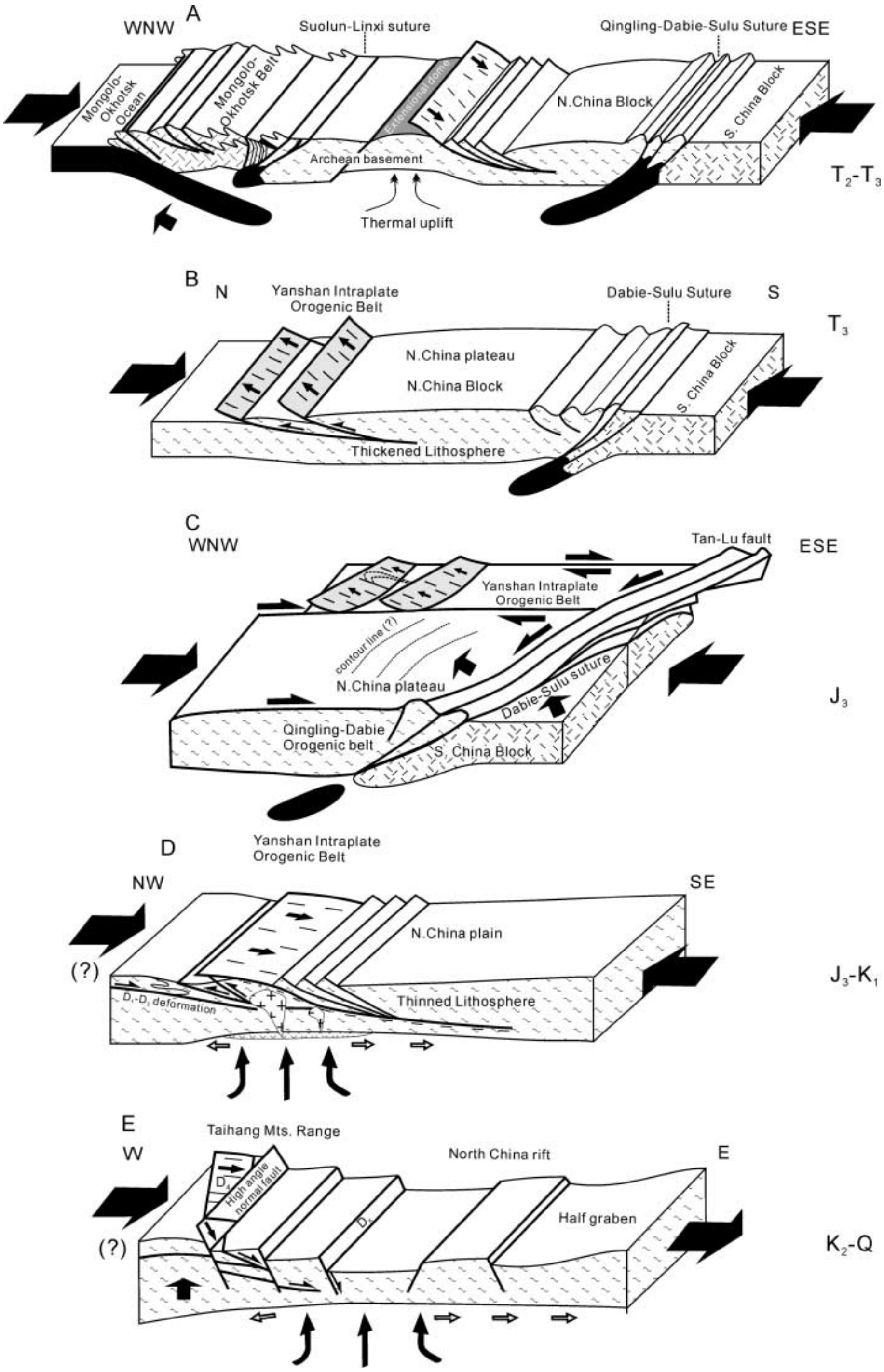


**Fig. 10.** A schematic diagram showing the tectonic evolution of the Yanshan intraplate orogenic belt (see text for additional references). (**a**) SE-directed subduction of the Mongolo-Okhotsk oceanic plate and the collision between the South and North China Blocks along the Qingling–Dabie–Sulu suture during the mid- to late Triassic. The subduction of the Mongolo-Okhotsk oceanic plate was associated with anatexis and uplift thermal flow underneath the North China Block. This is primarily responsible for the SE-directed extensional tectonics within the North China Block where a belt of extensional domes ($D_1$) developed. (**b**) The collision and continued compression of the South China Block into the North China Block resulted in extensive north–south crustal shortening and consequent intra-continental deformation, including NNW-directed thrusting within the Yanshan intraplate orogenic belt of this paper ($D_2$). (**c**) Indentation of the South China Block into the North China Block along the Dabie–Sulu suture created the sinistral Tan–Lu fault, and resulted in the WNW-directed movement of the southern North China Block and ESE-directed extrusion of the Yanshan belt. This oblique convergence was associated with a WNW-directional principal stress, consistent with that of the Nandazai thrust ($D_3$). (**d**) Extensive magmatic intrusions occurred within the Yanshan intraplate orogenic belt during late Jurassic to early Cretaceous time because of the collapse and thinning of the lithosphere ($D_4$). (**e**) The Taihang mountain range was uplifted in the Cenozoic because of extensional tectonics ($D_5$).

*dian Area*. Unpublished report (in Chinese).

Black, L.P., Kamo, S.I., Aleiikoff, J.N., Davis, D.W., Korsch, R.L. & Foudoulis, C. 2003. TEMORA 1: a new zircon standard for Phanerozoic U–Pb geochronology. *Chemical Geology*, **200**(1-2), 155–170.

Chavagnac, V., Jahn, B.M., Villa, I.M., Whitehouse, M.J. & Liu, D. 2001. Multichronometric evidence for an in situ origin of the ultrahigh pressure metamorphic terrane of Dabieshan, China. *Journal of Geology*, **109**, 633–646.

Chen, A. 1998. Geometric and kinematic evolution of basement-core structures: intraplate orogenesis within the Yanshan Orogen, northern China. *Tectonophysics*, **292**, 17–42.

Chen, X.B. 1999. Preliminary knowledge on control of Malanyu metamorphic core complex on metallization. *Geological Exploration Non-Ferrous Metals*, **8**, 311–324 (in Chinese with English abstract).

Compston, W., Williams, I.S. & Meyer, C. 1984. U–Pb geochronology of zircons from Lunar Breccia 73217 using a sensitive high mass-resolution ion microprobe. *Journal of Geophysical Research*, **89**, 525–534.

Darby, B.J. & Ritts, B.D. 2002. Mesozoic contractional deformation in the middle of the Asian tectonic collage: the intraplate Western Ordos fold–thrust belt, China. *Earth and Planetary Science Letters*, **205**, 13–24.

Darby, B.J., Davis, G.A. & Zheng, Y.D. 2001. Structural evolution of the southwestern Daqing Shan, Yinshan belt, Inner Mongolia, China. *In:* Hendrix, M.S. & Davis, G.A. (eds) *Paleozoic and Mesozoic Tectonic Evolution of Central and Eastern Asia: from Continental Assembly to Intracontinental Deformation*. Geological Society of America, Memoirs, **194**, 199–214.

Davis, G.A. 2003. The Yanshan belt of north China: tectonics, adakitic magmatism, and crustal evolution. *Earth Science Frontiers*, **10**, 373–384.

Davis, G.A., Qian, X., Zheng, Y. & Yu, H. 1989. The Shihetang thrust plate, a major crystalline nappe in the Yunmen mountains, Beijing, northeastern China. *Geological Society of America, Abstracts and Programs*, **21**, A319.

Davis, G.A., Qian, X. & Zheng, Y. et al. 1996. Mesozoic deformation and plutonism in the Yunmeng Shan: a Chinese metamorphic core complex north of Beijing, China. *In:* Yin, A. & Harrison, T.M. (eds) *The Tectonics Evolution of Asia*. Cambridge University Press, Cambridge, 253–280.

Davis, G.A., Wang, C., Zheng, Y., Zhang, J., Zhang, C. & Gehrels, G.E. 1998. The enigmatic Yinshan fold- and thrust-belt of northern China: new views on its intraplate contractional styles. *Geology*, **26**, 43–46.

Davis, G.A., Zheng, Y.D., Wang, C., Darby, B.J., Zhang, C. & Gehrels, G. 2001. Mesozoic tectonic evolution of the Yanshan fold and thrust belt, with emphasis on Hebei and Liaoning provinces, northern China. *In:* Hendrix, M.S. & Davis, G.A. (eds) *Paleozoic and Mesozoic Tectonic Evolution of Central and Eastern Asia: from Continental Assembly to Intracontinental Deformation*. Geological Society of America, Memoirs, **194**, 171–192.

Davis, G.A., Darby, B.J., Zheng, Y.D. & Spell, T.L. 2002. Geometric and temporal evolution of an extensional detachment fault, Hohhot metamorphic core complex, Inner Mongolia, China. *Geology*, **30**, 1003–1006.

Enkin, R., Yang, Z.Y., Chen, Y. & Courtillot, V. 1992. Paleomagnetic constraints on the geodynamic history of the major blocks of China from the Permian to the present. *Journal of Geophysical Research*, **97**, 13953–13989.

Fan, Q.-C. & Hooper, P.R. 1991. The Cenozoic basaltic rocks of eastern China: petrology and mineral composition. *Journal of Petrology*, **32**, 765–810.

Fan, W.M., Guo, F. & Wang, Y.J. 2003. Late Mesozoic calc-alkaline volcanism of post-orogenic extension in the northern Da Hinggan Mountains, northeastern China. *Journal of Volcanology and Geothermal Research*, **121**(1-2), 115–135.

Faure, M. & Natlin, B. 1992. The geodynamic evolution of the Eastern Eurasian margin in Mesozoic times. *Tectonophysics*, **208**, 397–411.

Fu, Z.Y. 1999. The metamorphic core complexes in Hebei, China. *Geology and Mineral Resources Research*, **14**, 10–16 (in Chinese with English abstract).

Ge, M. & Ren, J. 1990. Thrust tectonics in Western Hills of Beijing. *In:* Zhang, J. & Shan, W. (eds) *Study of Geology in Western Hills of Beijing*. China University of Geosciences Press, Wuhan, 30–41 (in Chinese with English abstract).

Gilder, S.A., Keller, G.R., Luo, M. & Goodell, P.C. 1991. Timing and spatial distribution of rifting in China. *Tectonophysics*, **197**, 25–243.

Guo, H.Q. 1985. Petrological characteristics and origin of gneissic rocks along northern flank of Fangshan pluton, Beijing. *Bulletin of the Institute of Geology–Chinese Academy of Geological Sciences*, **13**, 105–130 (in Chinese with English abstract).

Hacker, B.R., Ratschbacher, L., Webb, L., Ireland, T., Walker, D. & Dong, S.W. 1998. U/Pb zircon ages constrain the architecture of the ultrahigh-pressure Qinling–Dabie Orogen, China. *Earth and Planetary Science Letters*, **161**, 215–230.

Han, B.F., Zheng, Y.D., Gan, J.W. & Chang, Z.S. 2001. The Louzidian normal fault near Chifeng, Inner Mongolia: master fault of the quasi-metamorphic core complex. *International Geological Review*, **43**, 254–264.

Hebei Bureau of Geology 1989. *Regional Geology of Hebei Province*. Ministry of Geology and Mineral Resources, Geological Memoirs, Series 1, **25**, (in Chinese with English abstract).

Hebei Bureau of Geology 1990. *Metamorphic map of Hebei province, Beijing and Tianjing municipalities and its explanatory notes, China*. Geological Publishing House, Beijing, 1–40.

Ho, T.L. 1936. *The granitic intrusions of the Western Hills of Beiping*. Book Series of Geological Institute, Central Academy, **5**, 1–15.

Holk, G.J. & Taylor, H.P. 1997. O-18/O-16 homogenization of the middle crust during anatexis: the Thor–Odin metamorphic core complex, British Columbia. *Geology*, **25**, 31–34.

Kusky, T.M., Li, J.H., Glass, A. & Huang, X.N. 2004. Origin and emplacement of Archean ophiolites of the Central Orogenic belt, North China Craton. *In:* Kusky, T.M. (ed.) *Precambrian Ophiolites and Related Rocks*. Developments in Precambrian Geology, **13**, 223–274.

Lei, S.H., Hu, S.J., Zhao, Z.Y., Jiang, X.W. & Wang, S.D. 1994. Structures and mechanisms of the Fuping and Zanfang metamorphic core complexes in Hebei province. *Journal of Hebei Geological College*, **17**, 54–64 (in Chinese with English abstract).

Liaoning Bureau of Geology and Mineral Resources 1989. *Regional Geology of Liaoning Province*. Ministry of Geology and Mineral Resources, Geological Memoirs, Series 1, **14**, (in Chinese with English abstract).

Little, T.A., Holcombe, R.J., Gibson, G.M., Offler, R., Gans, P.B. & McWilliams, M.O. 1992. Exhumation of Late Palaeozoic blueschists in Queensland, Australia, by extensional faulting. *Geology*, **20**, 231–234.

Liu, G.H. & Wu, J.S. 1987. Metamorphic zones of the Fangshan area in Beijing. *Bulletin of the Chinese Academy of Geological Sciences*, **16**, 113–136 (in Chinese with English abstract).

Ludwig, K.R. 2001. *Squid 1.02. A User's Manual*. Berkeley Geochronological Center Special Publications, **2**, 1–19.

Luo, Z.K., Miao, L.C., Guan, K., Qiu, Y.S., Qiu, Y.M., McNaughton, N.J. & Groves, D.I. 2003. SHRIMP U–Pb zircon dating of the Dushan granite batholith and related granite–porphyry dyke, eastern Hebei province, China, and their geological significance. *Geochimica*, **32**, 173–180.

Martin, G.M. 2003. Basement-involved thrust faulting in a thin-skinned fold-and-thrust belt, Death Valley, California, USA. *Geology*, **31**, 31–34.

Meng, Q.R. 2003. What drove late Mesozoic extension of the northern China–Mongolia tract? *Tectonophysics*, **369**, 155–174.

Meng, Q.R., Hu, J.M., Jin, J.Q., Zhang, Y. & Xu, D.F. 2003. Tectonics of the late Mesozoic wide extensional basin system in the China–Mongolia border region. *Basin Research*, **15**, 397–415.

Nie, S.Y., Rowley, D.B. & Ziegler, A.M. 1990. Constraints on the locations of Asian microcontinents in Palaeo-Tethys during the late Palaeozoic. *In:* McKerrow, W.S. & Scotese, C.R. (eds) *Palaeozoic Palaeogeography and Biogeography*. Geological Society, London, Memoirs, **12**, 397–405.

Niu, S.G., Sun, E.Q., Xu, Z.S., Luo, D.W., Shao, Z.G. & Li, R. 1994. Fuping and Zanfang domes are Mesozoic to Cenozoic metamorphic core complexes within Taihang Mountains. *Geological Science and Technology Information*, **13**, 15–16 (in Chinese).

Ramsay, J.G. & Huber, M.I. 1987. *The Techniques of Modern Structural Geology—Volume 2: Fold and Fracture*. Academic Press, New York, 347–363.

Ren, J., Chen, T., Niu, B., Liu, Z. & Liu, F. 1990. *Tectonic Evolution of the Continental Lithosphere and Metallogeny in Eastern China and Adjacent Area*. Science Publishing House, Beijing, (in Chinese with English abstract).

Ren, J., Tamaki, K., Li, S. & Zhang, J. 2002. Late Mesozoic and Cenozoic rifting and its dynamic setting in Eastern China and adjacent areas. *Tectonophysics*, **344**, 175–205.

Richard, F.L. 1991. Role of crustal thickening and extensional collapse in the tectonic evolution of the Sevier–Laramide orogeny, western United States. *Geology*, **19**, 1104–1107.

Robert, J.T. 1998. Coseismic growth of basement-involved anticlines: the Northridge–Laramide connection. *Geology*, **26**, 335–338.

Shan, W., Song, H., Fu, Z. & Ren, J. 1991. *Principles, Methods and Practices of Structural Analysis*. China University of Geosciences Press, Wuhan (in Chinese).

Song, H. 1996. Characteristics of Fangshan Metamorphic Core Complex, Beijing and a discussion about its origin. *Geoscience Journal of Graduate School, China University of Geosciences*, **10**, 147–158 (in Chinese with English abstract).

Song, H. & Ge, M. 1984. The Indosinian movement in Western Hills of Beijing discussed in the light of the structural characteristics. *Geological Review*, **30**, 77–80 (in Chinese with English abstract).

Song, H., Fu, Z. & Yan, D.P. 1996. Extensional Tectonics and Metamorphic Core Complex of Western Hills. *Beijing: Field Trip Guide for 30 IGC*, T210, 1–8.

Stacey, J.S. & Kramers, J.D. 1975. Approximation of terrestrial lead isotope evolution by a two-stage model. *Earth and Planetary Science Letters*, **26**, 207–221.

Timothy, P. & Stephen, M. 1999. Origin of the Uinta recess, Sevier fold–thrust belt, Utah: influence of basin architecture on fold–thrust belt geometry. *Tectonophysics*, **312**, 203–216.

Van der Voo, R., Spakman, W. & Bijwaard, H. 1999. Mesozoic subduction slabs under Siberia. *Nature*, **397**, 246–249.

Wang, Q. & Liu, X.Y. 1986. Paleoplate tectonics between Cathaysia and Angaraland in Inner Mongolia of China. *Tectonics*, **5**, 1073–1088.

Wang, Q., Liu, X.Y. & Li, Q.Y. 1990. *Plate Tectonics between Cathaysian (S. China) and Angola Paleo-continent—Plate Tectonics Evolution of North China*. Beijing University Press, Beijing.

Wang, Y. 1996. *Tectonic Evolutional Process of Inner Mongolia–Yanshan Orogenic Belt in Eastern China During the Late Palaeozoic–Mesozoic*. Geological Publishing House, Beijing (in Chinese with English abstract).

Wei, B. & Song, H. 1990. Fangshan metamorphic core complex, Beijing. *In:* Zhang, J. & Shan, W. (eds) *Study of Geology in Western Hills of Beijing*. China University of Geosciences Press, Wuhan, 42–47 (in Chinese).

Wong, W.H. 1929. The Mesozoic orogenic movement in eastern China. *Geological Society of China Bulletin*, **8**, 33–44.

Xiao, W.J., Windley, B.F., Hao, J. & Zhai, M.G. 2003. Accretion leading to collision and the Permian Solonker suture, Inner Mongolia, China: termination of the central Asian orogenic belt. *Tectonics*, **22**, 1–20.

Yan, D.P., Zhou, M.F., Song, H.L., Wang, X.W. & Malpas, J. 2003. Origin and tectonic significance of a Mesozoic multi-layer over-thrust system within the Yangtze Block (South China). *Tectonophysics*, **361**, 239–254.

Yin, A. & Nie, S.Y. 1996. A Phanerozoic palinspastic reconstruction of China and its neighboring regions. *In:* Yin, A. & Harrison, M. (eds) *The Tectonic Evolution of Asia*. Cambridge University Press, Cambridge, 442–485.

Yu, W.L. & Zhang, J.M. 1996. Discussion on the genesis of Dushan granite in eastern Hebei, Northern China. *Journal of Mineral Petrology*, **16**, 1–7 (in Chinese with English abstract).

Zhang, C. 1996. *Structural and tectonic study on the intracontinental orogenesis of the Yanshan orogenic belt in Mesozoic*. PhD thesis, China University of Geosciences, Beijing (in Chinese with English abstract).

Zhang, C., Song, H.L., Wang, G.H., Yan, D.P. & Sun, W.H. 2001. Mesozoic dextral strike-slip structural system in middle segment of intraplate Yanshan orogenic belt, Northern China. *Earth Science Journal of China University of Geosciences*, **26**, 464–472.

Zhang, J. & Li, Z. 1991. Deformational fabrics and ballooning intrusion mechanism of Fangshan granodiorite, Beijing. *In:* Zhang, J. & Shan, W. (eds) *Study of Geology in Western Hills of Beijing*. China University of Geosciences Press, Wuhan, 48–56.

Zhang, K.J. 1997. North and South China collision along the eastern and southern North China margins. *Tectonophysics*, **270**, 145–156.

Zhang, Q., Wang, Y. & Wang, Y.L. 2001. Preliminary study on the components of the lower crust in east China Plateau during Yanshanian Period: constraints on Sr and Nd isotopic compositions of adakite-like rocks. *Acta Petrologica Sinica*, **17**, 505–513.

Zhang, Q.S., Yang, Z.S., Gao, D.Y. & Ren, H.M. 1991. *Geology and Gold Deposit in the High-grade Metamorphic Area of Jinchangyu, Eastern Hebei*. Geological Publishing House, Beijing (in Chinese).

Zhang, Z.M., Liou, J.G. & Coleman, R.G. 1984. An outline of the plate tectonics of China. *Geological Society of America Bulletin*, **95**, 295–312.

Zhao, X.X., Coe, R.S., Zhou, Y.X., Wu, H.R. & Wang, J. 1990. New paleomagnetic results from North China: collision and suturing with Siberia and Kazakhstan. *Tectonophysics*, **181**, 43–81.

Zheng, Y., Wang, Y., Liu, R. & Shao, J. 1988. Sliding–thrusting tectonics caused by thermal uplift in the Yunmen Mountains, Beijing, China. *Journal of Structural Geology*, **2**, 135–144.

Zorin, Y.A. 1999. Geodynamics of the western part of the Mongolia–Okhotsk collisional belt, Trans-Baikal region (Russia) and Mongolia. *Tectonophysics*, **306**, 33–56.

Received 30 November 2004; revised typescript accepted 17 June 2005.
Scientific editing by Rob Strachan